SUPPLEMENTARY INFORMATION

During the thermal treatment, the pellets from the different precursors were treated at the same temperature (T = 1350 ºC) but with different treatment duration; 10 hours for the commercial powder based precursors, samples *c*Lix, and 15 hours for the ones starting from nanoparticles doped with Lithium, referred to as *np*Lix samples, in both cases 0<x<30 % cationic. With these experimental conditions the density of structures grown on the pellets is comparable for both series, as observed in Figure S1.

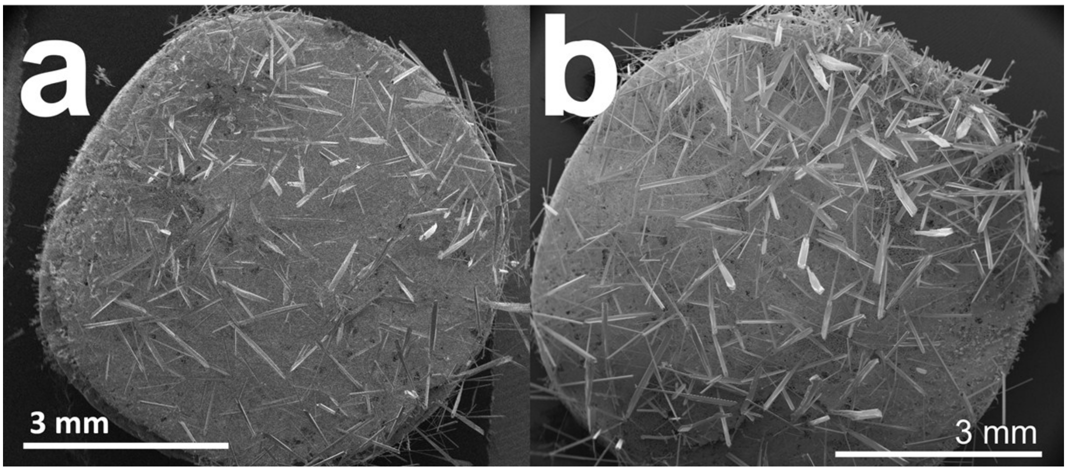

Fig S1. SnO_2 pellets after the corresponding thermal treatment. Comparable density of microstructures growing on the pellet surface is observed for sample a) npLi30 and b) cLi30.

In order to investigate the crystalline orientation of the lateral faces and the growth direction of these microtubes, EBSD and Raman spectroscopy have been used. The crystallographic orientation of the lateral surfaces that define the microstructures can be identified with EBSD measurements in a SEM. The microtubes were carefully detached from a pellet and placed onto a Si (100) substrate, in this way we can assure a correct configuration for the measurement. The Figure S2 (a-d) shows the indexed EBSD pattern formed by the corresponding Kikuchi lines, the pole figure, the secondary electron image of the probed region of a microtube and a ball model of the microstructure, respectively. The probed face of the microtube corresponds to the (110) plane of rutile SnO_2. In agreement with the XRD results, no differences have been found for the crystalline orientation of the lateral faces of the measured microstructures independently of the precursors or dopant concentration used. According to these results, the {110} planes, which show the lowest energy surface compared with other faces in the rutile system,[1, 2] form the single crystalline faces of these structures.

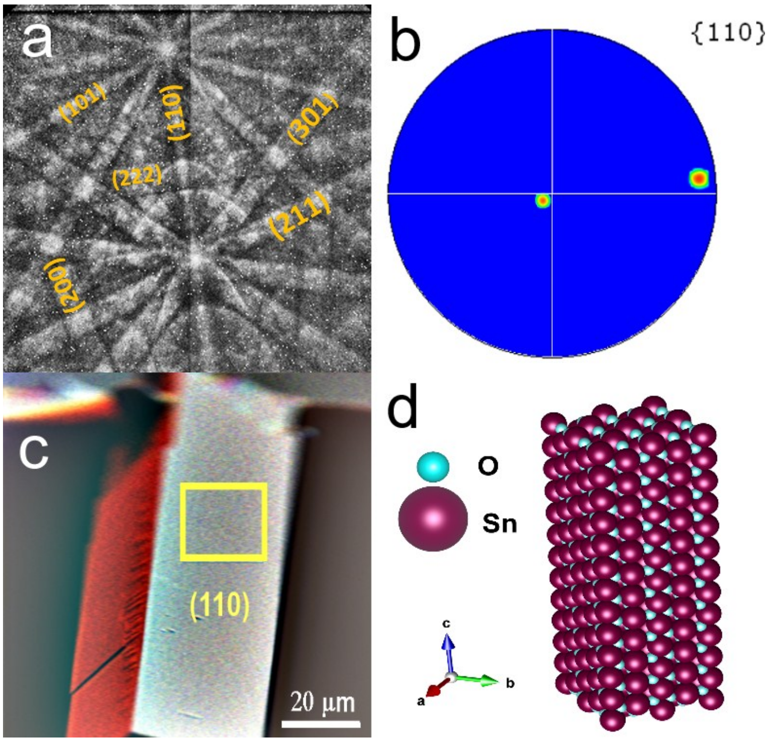

Fig. S2. (a) EBSD pattern with indexed reflections, (b) polar configuration of a probed tube face, (c) SE image of the microtube on the squared area corresponding with the (110) plane (d) ball model representation of a rod with {110} lateral faces.

In order to determine the growth direction of these anisotropic structures polarized Raman spectroscopy was carried out using a laser of $\lambda = 325\ nm$. The microtubes exhibit the main signatures of the Raman spectra of cassiterite SnO_2 as shown in Figure S3a) for the *np*Lix samples. The main actives modes [3] are identified as the E_g (476 cm^{-1}), A_{1g} (638 cm^{-1}), B_{2g} (782 cm^{-1}) and the A_{2u} (~700 cm^{-1}) longitudinal optical mode, showing no differences in the position of the peaks or their relative intensity when the concentration of lithium is increased as is shown in S3 (a-b). However, significant differences in the spectra appear when two different configurations of the laser polarization, in Porto notation,[4, 5] -Y(XX)Y and -Y(ZZ)Y, (with the laser polarization orthogonally ($\delta = 0°$) and parallel ($\delta = 90°$) to the microtube axis, respectively) are used for Raman measurements (Figure S4). These differences confirm the high sensitivity of the B_{2g} mode to the laser polarization. When the laser polarization is parallel to the microtube growth axis -Y(XX)Y, ($\delta = 90°$), the doped tubes have a dominant A_{1g} mode, while the mode B_{2g} is quenched, which indicates a [001] growth direction, in agreement with the results obtained for TiO_2 microtubes with rutile crystalline structure and analogous morphology.[6] These results are in agreement with the XRD and EBSD results. The modes A_{1g} and B_{2g} are related to the Sn-O stretching comprising motions of the O anions with respect to the Sn cations, symmetrically or asymmetrically, orthogonally to the c axis of the microtube. Another translational mode, E_g, which involves the motion of O anions along the c axis, is hardly observed compared to the more intense A_{1g} and B_{2g} modes. In the region of ~700 cm^{-1}, the slight variation in the relative intensity, larger for the $\delta = 0°$ configuration, could be associated with the IR active A_{2u} LO mode in SnO_2.[7, 8] Although doping usually could cause shifts and broadening of the Raman peaks, such as those reported for SnO_2 doped with Fe,[9] no significant intensity differences or any shift in the Raman modes due to the different Li concentrations are observed in the Raman spectra of the microtubes.

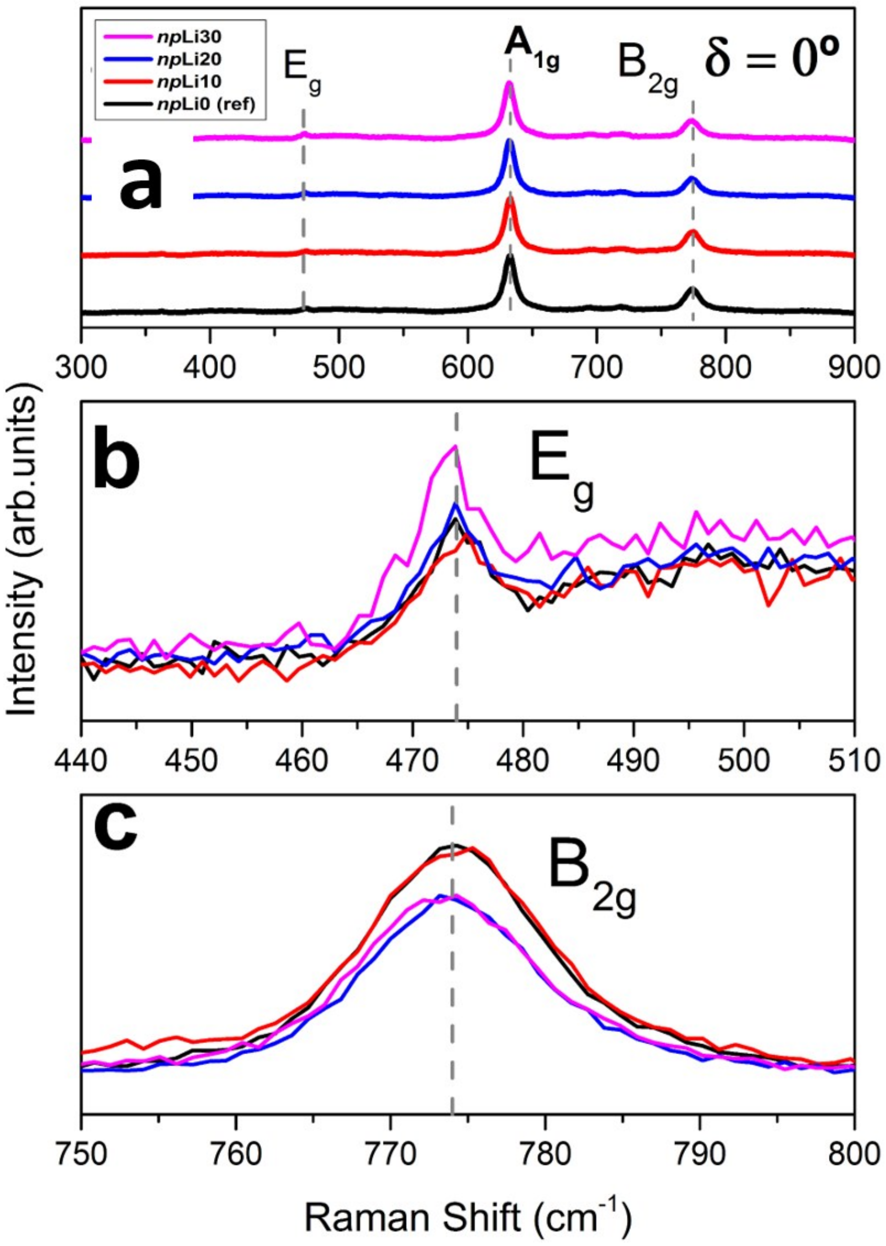

Fig. S3. a) Raman spectra for npLix samples with different nominal Li concentration. Dashed lines mark the main active modes in Cassiterite SnO_2. b) Detail of the E_g and c) B_{2g} mode peaks.

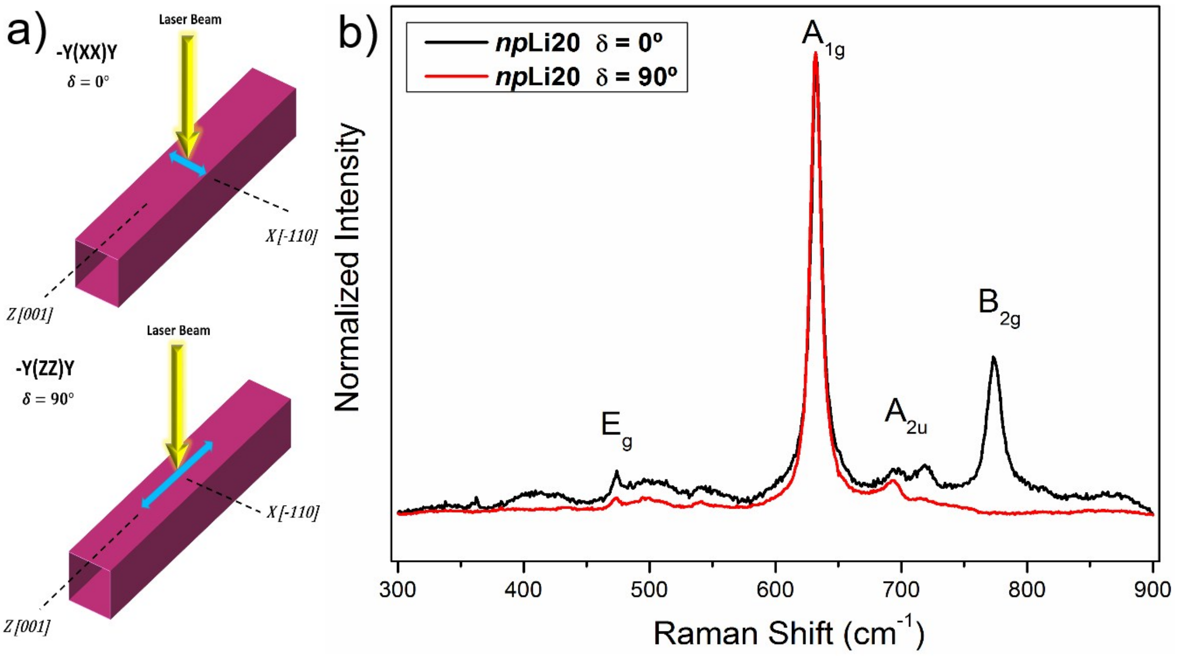

Fig. S4. a) Porto notation for a microtube and b) polarized Raman spectra on a microtube of npLi20

References:

1. P. A. Mulheran and J. H. Harding, *Modelling and Simulation in Materials Science and Engineering*, 1992, **1**, 39.
2. P. A. Bhatt, S. Mishra, P. K. Jha and A. Pratap, *Physica B: Condensed Matter*, 2015, **461**, 101-105.
3. A. Dieguez, A. Romano-Rodrıguez, A. Vila and J. Morante, *Journal of Applied Physics*, 2001, **90**, 1550-1557.
4. S. Porto, P. Fleury and T. Damen, *Physical Review*, 1967, **154**, 522.
5. V. Presser, B. E. Schuster, M. Casu, U. Heinemeyer, F. Schreiber, K. Nickel and T. Chasse, *Journal of Raman Spectroscopy*, 2009, **40**, 2015-2022.
6. G. C. Vasquez, M. A. Peche-Herrero, D. Maestre, A. Cremades, J. Ramirez-Castellanos, J. M. Gonzalez-Calbet and J. Piqueras, *CrystEngComm*, 2013, **15**, 5490-5495.
7. L. Abello, B. Bochu, A. Gaskov, S. Koudryavtseva, G. Lucazeau and M. Roumyantseva, *Journal of Solid State Chemistry*, 1998, **135**, 78-85.
8. W. Zhou, R. Liu, Q. Wan, Q. Zhang, A. L. Pan, L. Guo and B. Zou, *The Journal of Physical Chemistry C*, 2009, **113**, 1719-1726.
9. X. Mathew, J. Enriquez, C. Mejia-Garcia, G. Contreras-Puente, M. Cortes-Jacome, J. T. Antonio, J. Hays and A. Punnoose, *Journal of applied physics*, 2006, **100**, 073907.